A CF$_4$ based positron trap

You may also be interested in:

Monte Carlo modeling and optimization of buffer gas positron traps
Sran Marjanovi and Zoran Lj Petrovi

Ultra-low energy antihydrogen
M H Holzscheiter and M Charlton

Methods and progress in studying inelastic interactions between positrons and atoms
R D DuBois

Experimental studies of positrons scattering in gases
M Charlton

Positron cooling by vibrational and rotational excitation of molecular gases
M R Natisin, J R Danielson and C M Surko

A trap-based positron beamline for the study of materials
J P Sullivan, J Roberts, R W Weed et al.

Spatial profiles of positrons injected at low energies into water: influence of cross section models
Wade J Tattersall, Daniel G Cocks, Gregory J Boyle et al.

Positron extraction to an electromagnetic field free region
D A Cooke, G Barandun, S Vergani et al.

A CF$_4$ based positron trap

Srdjan Marjanović[1], Ana Banković[1], David Cassidy[2], Ben Cooper[2], Adam Deller[2], Saša Dujko[1] and Zoran Lj Petrović[1,3]

[1] Institute of Physics, University of Belgrade, Pregrevica 118, 11080 Belgrade, Serbia
[2] Department of Physics and Astronomy, University College London, Gower Street, London WC1E 6BT, UK
[3] Serbian Academy of Sciences and Arts, Knez Mihajlova 35, 11000 Belgrade, Serbia

E-mail: msrdjan@ipb.ac.rs

CrossMark

Abstract

All buffer-gas positron traps in use today rely on N$_2$ as the primary trapping gas due to its conveniently placed a $^1\Pi$ electronic excitation cross-section. The energy loss per excitation in this process is 8.5 eV, which is sufficient to capture positrons from low-energy moderated beams into a Penning-trap configuration of electric and magnetic fields. However, the energy range over which this cross-section is accessible overlaps with that for positronium (Ps) formation, resulting in inevitable losses and setting an intrinsic upper limit on the overall trapping efficiency of ∼25%. In this paper we present a numerical simulation of a device that uses CF$_4$ as the primary trapping gas, exploiting vibrational excitation as the main inelastic capture process. The threshold for such excitations is far below that for Ps formation and hence, in principle, a CF$_4$ trap can be highly efficient; our simulations indicate that it may be possible to achieve trapping efficiencies as high as 90%. We also report the results of an attempt to re-purpose an existing two-stage N$_2$-based buffer-gas positron trap. Operating the device using CF$_4$ proved unsuccessful, which we attribute to back scattering and expansion of the positron beam following interactions with the CF$_4$ gas, and an unfavourably broad longitudinal beam energy spread arising from the magnetic field differential between the source and trap regions. The observed performance was broadly consistent with subsequent simulations that included parameters specific to the test system, and we outline the modifications that would be required to realise efficient positron trapping with CF$_4$. However, additional losses appear to be present which require further investigation through both simulation and experiment.

(Some figures may appear in colour only in the online journal)

1. Introduction

Since production of the first slow positron beams in the 1970s [1] significant technological improvements have occurred [2, 3]. The state of the art for radioactive-source-based beams allows for the generation of low-energy beam currents of around $10^7 e^+/s$ (i.e., ∼1 pA) using solid-neon moderators [4]. Although a wide variety of experiments can be performed with such beams, the availability of positrons is still a limiting factor in some areas. For example, much progress has been made in experimental positron scattering from atoms and molecules [5] but comparable electron scattering work is considerably more advanced [6], in part because high-quality beams with currents of μA or more can easily be generated.

The development of buffer-gas positron traps by Surko and co-workers in the late 1980s [7, 8] has greatly advanced the field of low-energy positron physics. Recent implementations and variations of the trapping apparatus [9–13] have allowed for new experiments using, for example, positrons with high energy resolution ($<$50 meV) or the generation of intense pulsed beams with instantaneous currents of up
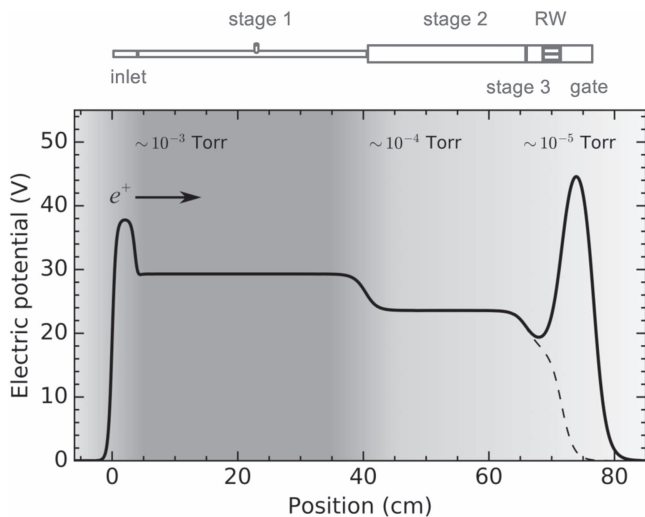
Figure 1. The basic structure of a 'two-stage' Surko trap, with an applied three-stage potential well and the associated buffer-gas pressures. The dashed line indicates the electric potential during particle ejection. The shading represents the pressure in each stage.
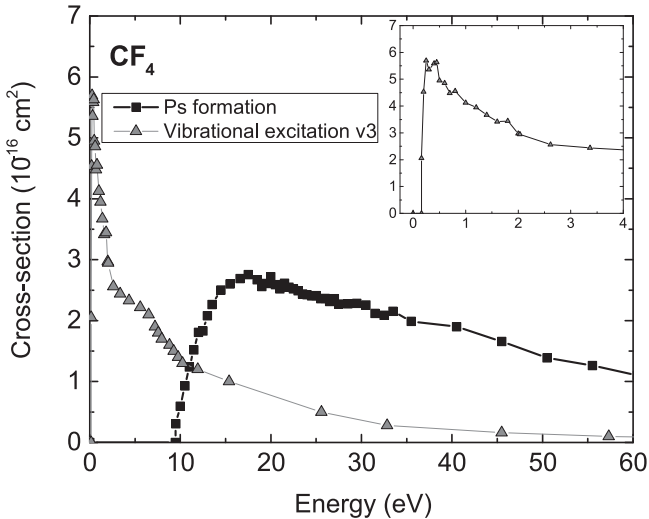

Figure 2. Measured cross-sections for Ps formation and electronic excitation by positrons with molecular nitrogen. The data are taken from [14]. Also shown are the approximate energy spreads expected for beams derived from tungsten moderators (solid black bar) and solid-neon moderators (dashed grey bar).

to 10 mA. Positron traps have thus made possible highly accurate measurements of scattering cross-sections for positron–matter interactions [14–17], creation of positronium (Ps) molecules [18], formation of antihydrogen atoms [19–21], and Ps-laser spectroscopy [22], and may eventually lead to the creation of a Ps Bose–Einstein condensate [23]. Positron scattering data and theoretical cross-section calculations have enabled swarm simulations and calculation of transport parameters of positrons in various gasses [24–29]. In turn, these have facilitated simulations of buffer-gas positron trap operation [30], providing insight into the underlying trapping mechanisms, as well as suggesting potential ways to improve the trapping efficiency, thermalisation time, and beam compression.

The Surko positron trap is essentially a Penning trap: axial confinement of the charged particles is achieved using an electric potential minimum (along *z*), which is co-axial with a magnetic field for radial confinement. Buffer gas is admitted into the electrodes, which are cylindrical and of varying lengths and radii. The electrode geometry results in a pressure gradient that varies over several orders of magnitude. The first (trapping) stage is at the highest pressure of 10^{-3} Torr, while the gas pressure in the last (accumulation) stage is typically around 10^{-5}–10^{-6} Torr. An electric potential is applied across the electrode structure such that positrons experience deeper potential wells as they are captured and cooled into the final stage of the trap, as shown in figure 1. The original Surko design comprised three stages of different electrode radii [9] and is capable of accumulating many positrons ($>10^8\, e^+$). More recently, compact two-stage traps have also been used for their lower space requirements and cost [11, 31], and although the maximum output per cycle is limited to approximately $10^6\, e^+$, they are well suited to a wide range of experiments. Note that here 'two-stage' refers to the electrode structure and pressure differential of the trap;
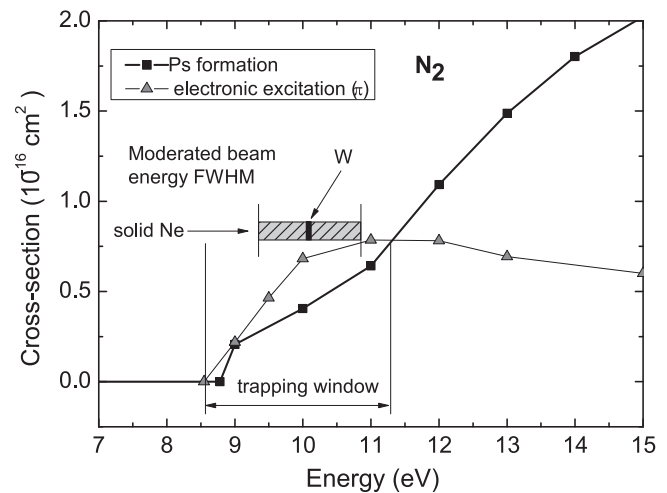
the electric potential well usually forms three distinct stages, as shown in figure 1.

Currently, most (but not all: e.g., [32, 33]) positron trapping devices rely on inelastic $a^1\Pi$ electronic excitation of N_2 molecules. This process has a threshold of 8.5 eV, which is roughly the amount of energy that a positron loses in the process. After a single $a^1\Pi$ excitation event within the trap, positrons will no longer have enough energy to escape over the inlet electrode potential and are thus captured. A significant disadvantage of this approach, however, is that the electronic excitation threshold is close to the Ps formation threshold (see figure 2), resulting in unavoidable losses. Following several successive collisions with the buffer-gas molecules, positrons cool to the final stage of the trap. The electric potential difference between adjacent stages is tuned to optimise $a^1\Pi$ electronic excitations of N_2, so as to efficiently transfer positrons to this region. A small amount of gas with a strong vibrational excitation cross section (typically SF_6 or CF_4) is often added to increase the positron cooling rate in the final stage. Further cooling is possible via rotational excitations, for which N_2 has a larger cross section than, e.g., CF_4 [34–36].

Molecular nitrogen is used as the primary trapping gas because it is the only known molecule for which the threshold for electronic excitation (~8.5 eV) is sufficiently below that of Ps formation. As shown in figure 2, the Ps formation threshold for N_2 is ~8.8 eV and the cross-section remains below that for $a^1\Pi$ excitation up to ~11.5 eV. This leaves a trapping window in the 8.5–11.5 eV range where energy loss via electronic excitations (and hence trapping) can successfully compete with Ps formation [9]. Owing to the position, shape and magnitude of the relevant cross-sections, there is a probability of around 50% that positrons in the trapping window will undergo excitation rather than Ps formation [30]. This intrinsic limitation is relevant for capture and the initial cooling phase, resulting in efficiencies of $\lesssim 25\%$: reported

Figure 3. Measured cross-section for the strongest vibrational excitation channel and positronium formation in CF$_4$. The inset shows an expanded section of the vibrational excitation cross-section at low energy. The vibrational cross-section data are taken from [15]. Measured Ps formation cross-sections in CF$_4$ are unavailable, and the data shown are scaled Ar cross-sections, as explained in [42].

Figure 4. Modelled three stages of axial electric potential.

total efficiencies from different devices vary considerably, ranging from 5%–20% [11–13, 37].

Low-energy positron beams emitted from solid-neon, or other rare-gas moderators [4], are epithermal and therefore posses relatively large energy spreads (∼1.5 eV). Moderators that operate via work-function emission (for example tungsten [2]) will have considerably smaller energy spreads (∼75 meV [38]). A narrow energy spread makes it easier to tune the excitation-to-Ps-formation ratio more precisely, and thus can lead to an increased trap efficiency (up to 30% has been reported [9]). However, since solid-neon moderators are around an order of magnitude more efficient than tungsten moderators [2] it remains advantageous to use the former.

In this paper we consider a possible method of circumventing the intrinsic efficiency limit of N$_2$ based traps by using CF$_4$ as the principal trapping gas. Large cross-sections have been measured for vibrational excitation of CF$_4$ by positrons [15, 39], and this has motivated us (and others, e.g., [40]) to examine whether it is possible to trap positrons through vibrational losses on CF$_4$ molecules [41]. These are dominant in the 0.2–2 eV energy range, well below the threshold for Ps formation. However, the energy loss per collision (0.159 eV for the strongest vibrational channel of CF$_4$) is much smaller than for electronic excitation of N$_2$ (8.5 eV, see figures 2 and 3). Hence, instead of just one, several collisions are needed to capture positrons in the trap. The peak cross-section value for vibrational excitation of CF$_4$ is almost seven times larger than the N$_2$ electronic excitation cross-section [9, 15, 39], while the energy loss per event is roughly 50 times smaller. Thus, one can crudely estimate that a CF$_4$ based trap would operate with a gas pressure on the order of 7 times higher than N$_2$ traps; this estimate is consistent with the results of the simulations.
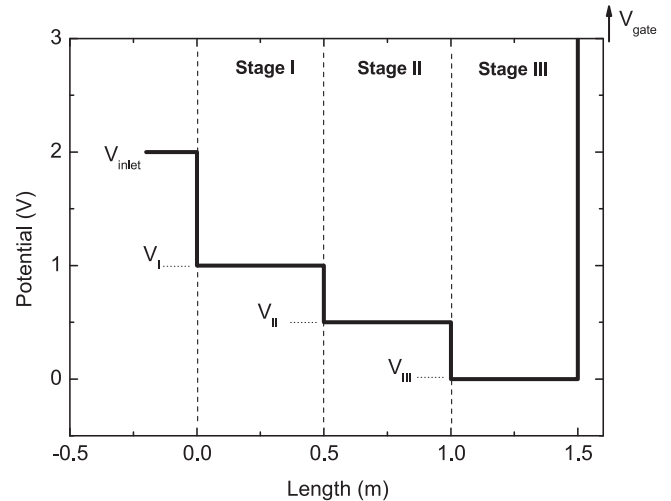
2. The model

To test the proposed scheme we model the traditional three-stage Surko trap structure. Each stage has a particular gas pressure and composition, axial magnetic field, electric potential, electrode radius and length. In the simulations the gas pressures in various regions is defined, and does not depend on the physical structure of the trap electrodes as it would in a real device. This means that the interplay between the positron scattering dynamics and the device geometry is controlled artificially, and the implementation of any real representation of simulated device parameters would have to take into account the true differential pumping requirements.

The trap has an inlet electrode whose potential is set somewhere below the incident beam energy, and a gate electrode with the potential set significantly above it, as shown in figure 1. Within each trapping stage the simulation assumes that there is no electric field, and the positrons exhibit cyclotron motion according to the applied magnetic field and the perpendicular beam energy. Upon crossing the boundary between stages positrons are either accelerated, decelerated, or reflected in the axial direction, depending on the individual particle energy and potential difference between the origin and destination stage. Positrons that reach the walls via radial transport, or have enough energy to cross the inlet potential after reflecting from the gate, are removed from the simulation.

The electric potential structure used in the model is shown in figure 4. The incident positron beam energy distribution is based on the ∼1.5 eV FWHM expected from a solid-neon moderator. For the purpose of the simulation we have assumed a triangular energy distribution, in which the initial velocity vector is uniformly distributed across 2π sr, with $v_z > 0$. We also include an offset in the beam energy that represents an electric bias applied to the source. The spatial distribution of the initial positrons is assumed to be uniform and 3 mm in diameter. We note that although the chosen distributions are generically representative, more realistic

**Table 1.** Parameters used in the CF$_4$ trap simulations.

Parameters	Stage I	Stage II	Stage III
Radius (mm)	5	20	20
Length (m)	0.5	0.5	0.5
Pressure (Torr)	10^{-3}	10^{-4}	10^{-5}
Buffer gas	CF$_4$	CF$_4$	N$_2$ + CF$_4$
Magnetic field (G)	530	530	530
Voltage (V)	1.0	0.5	0
Aditional parameters			
Inlet voltage(V)		2	
Source bias		0.1	
Starting energy FWHM (eV)		1.5	

Figure 5. Mean kinetic energy of positrons in each individual stage of a CF$_4$ trap as a function of time, and the mean energy of all particles in a CF$_4$ and an N$_2$ trap (total).

models of specific beam implementations are possible (e.g., a Gaussian energy profile or an annular beam profile [12, 13]).

The Monte Carlo simulation methodology employed includes a simplified description of the electric potential inside the trap. We assume that there is no electric field within individual stages, and that the energy gain from potential difference between electrodes is instantaneous. Therefore, the effects described in the simulations come, almost entirely, from scattering of positrons on the background gas. Also, the magnetic field is assumed to be perfectly axial, so any possible positron loss due to field misalignments (e.g., [9]) are not described in the simulation. Investigations of positron transport inside the trap, under imperfect field conditions will be the focus of future work.

The parameters used in the simulation (geometry, voltages, magnetic field strength and pressures) are given in table 1. All the simulation results described here were obtained using these parameters, unless stated otherwise. The chosen values (excluding the voltage settings) broadly reflect those of several current trap implementations, e.g., [10–13]. The parameter that has the most influence on trapping efficiency is the product of pressure and length of stage I, as it governs the amount of scattering a positron experiences in the trapping region.

The simulation includes pure CF$_4$ in stages I and II, and a 50% mixture of CF$_4$ and N$_2$ in stage III. Interactions between positrons and the ambient (300 K) background gas are described through the standard Monte Carlo technique [30, 43–45], including only binary collisions, and with a detailed treatment of thermal collisions [46]. In addition, superelastic collisions are included, with cross-sections defined through the principle of detailed balance. The cross-section data for positron interactions with CF$_4$ and N$_2$ have been compiled in [42], however, measured differential scattering data are not currently available. Therefore, we have assumed isotropic scattering (in the centre of mass inertial frame) for all types of collisions, unless otherwise stated. Between 10^4 and 10^6 positrons were simulated, with run times ranging from several hours to several days. Due to the low number density of positrons during the trapping process we neglect space-charge effects and any kind of collective phenomena. The trajectory of a positron between subsequent
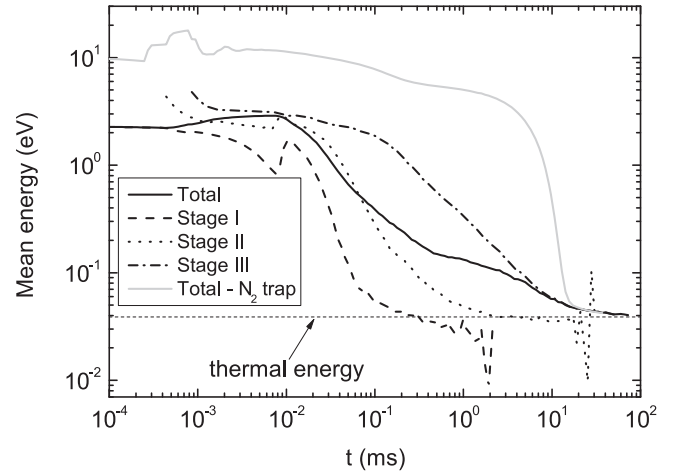
collisions is calculated analytically depending on the particle velocity and magnetic field.

The Monte Carlo code has been previously tested in electron swarm modelling, where binary collisions dominate the transport and thus benchmark calculations provide an excellent test of the representation of the physical processes. In addition, and more importantly for the present paper, the code has been tested for a number of situations where full equilibrium between energy gained from the field and lost in collisions is not reached. A number of kinetic phenomena are known to develop for electrons under these conditions [47], and the same is expected for positrons during the process of thermalisation. The present Monte Carlo methodology is thus well-suited to describe positrons in a buffer-gas trap.

3. Simulation results

The most important properties of a positron trap will depend, to some extent, on the application. For example, in the generation of intense pulses that will be bunched and implanted into a Ps-converter [13] the positron temperature is not a critical parameter, but the beam size is important. Conversely, for the production of high resolution beams [8] it is necessary to avoid heating the positrons, but as these are extracted axially the size of the plasma is less important. In general the most important characteristics are (1) the trapping efficiency, (2) the beam size and (3) the positron temperature. We have therefore extracted these parameters from the simulation.

The mean kinetic energy of positrons in the simulated devices (both N$_2$ and CF$_4$ based) was determined for each individual stage, and for the entire trap, as a function of time (see figure 5). These data indicate that the positron thermalisation process is quite different in a CF$_4$ trap than it is with N$_2$ [12, 30, 48]. This is mainly because the positrons enter the trap with much less energy, and because they spend more time in the first and the second stages where the pressure is higher. Nevertheless, in both cases positrons approach
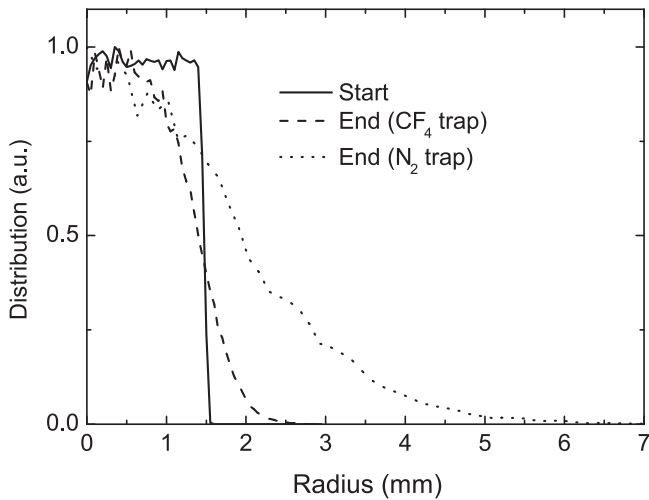
Figure 6. Simulated radial distributions of positrons as they enter the trap (start) and after thermalisation (end) in both a CF_4 and an N_2 based trap.

Figure 7. Total fraction of particles remaining in the trap as a function of time, and different loss processes.

Figure 8. The total number and the number of particles in each stage of a CF_4 trap during the thermalisation process.

thermal energies in approximately the same time scale. We note that figure 5 shows the *mean* positron energy, so at longer times positrons in stages I and II exhibit sub-thermal energies because of the low number of particles remaining.

An energetic positron beam entering a buffer-gas trap will tend to expand radially, primarily because of elastic collisions at higher energies [30]. In a CF_4 trap the incident positron energy is a few eV, much less than the $\sim$10 eV in an N_2 trap [9]. Therefore there is less energy available to be transferred, and the trapped beam will be narrower. In addition, due to the different thermalisation dynamics (see figure 5), particles spend less time in the third stage of the trap, and have less time to diffuse before thermalisation. As such, this trapping scheme is well suited to the rapid-cycle operation used in scattering experiments. These effects are highlighted in figure 6, which shows the simulated radial distributions of positrons in CF_4 and N_2 traps with the same geometry and gas pressures. In practice positron beams are often compressed using time-varying electric fields (i.e., the rotating-wall technique [13, 49]). These have not been included in the present simulation, but are expected to perform similarly in CF_4 and N_2 traps, as the composition of gas in stage III is similar.

The total efficiency of a positron trap depends on the particle capture rate and any loss mechanisms that may exist. The primary losses in the simulated trap are due to particles that do not experience enough inelastic collisions after reflection from the gate electrode. Ps formation, transport to the electrode walls, and direct annihilation are also included in the simulation, but are entirely negligible in the ideal CF_4 device. The simulated capture efficiency and loss mechanisms in the trap are shown in figure 7. We define the trap efficiency as the percentage of positrons passing the inlet electrode, that are trapped by the time the swarm thermalises.

Figure 8 shows the simulated distribution of positrons in separate trap stages during the thermalisation process, indicating the probability of finding a positron in a particular
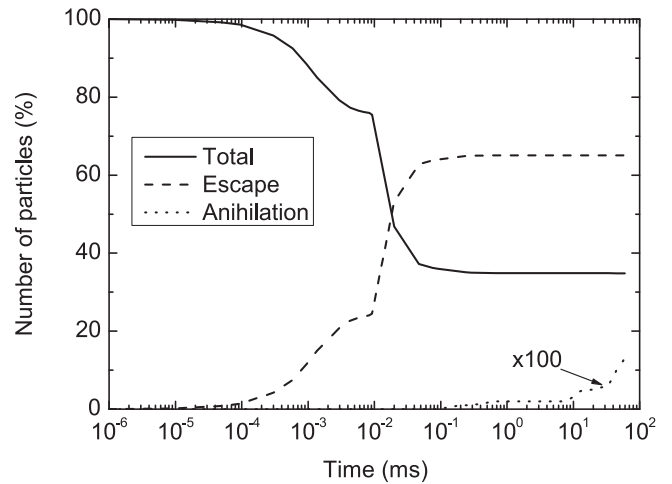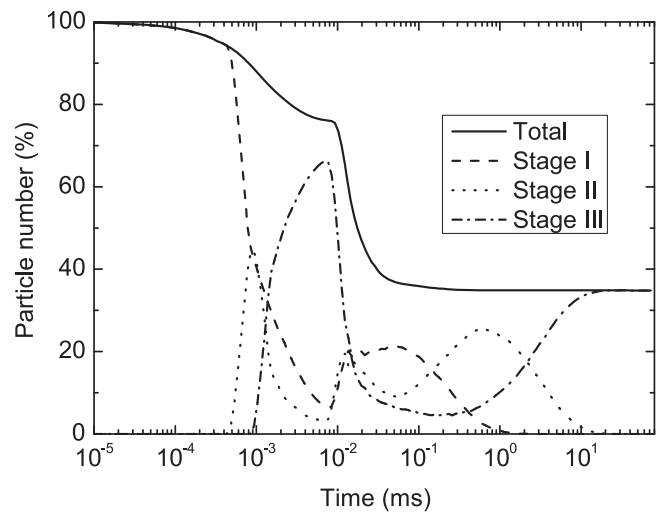
stage, after entering the device. This probability depends on the dynamics of the thermalisation process as well as the trap structure (see table 1). Thus, the apparent peak in S3 arises because this stage is effectively twice the length of S2, since the positrons are reflected back. We find that approximately 5% escape before the beam reaches the second stage due to backscattering collisions in the first. This figure must be treated with caution, however, because the required differential cross-section (DCS) data are not available. We discuss the implications of assuming isotropic DCS in section 4.

The data in figure 8 were obtained with a stage I pressure of 1 mTorr, which roughly corresponds to the stage I pressure in an N_2 trap. However, higher pressures will lead to an increased efficiency, as indicated in figure 9. These data show the simulated efficiency of the trap for different pressures, with up to 60% efficiency at 5 mTorr of CF_4. Even higher pressures cannot improve the trapping efficiency further, as all of the positrons experience enough collisions to be either
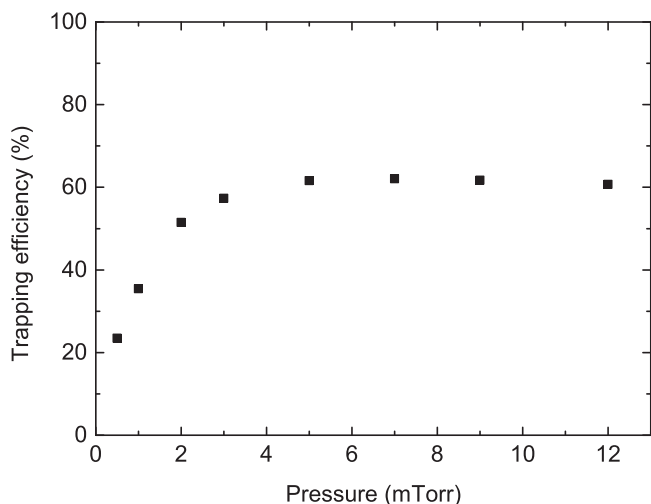
Figure 9. Simulated efficiency of the trap as a function of pressure of CF_4 in the first stage.
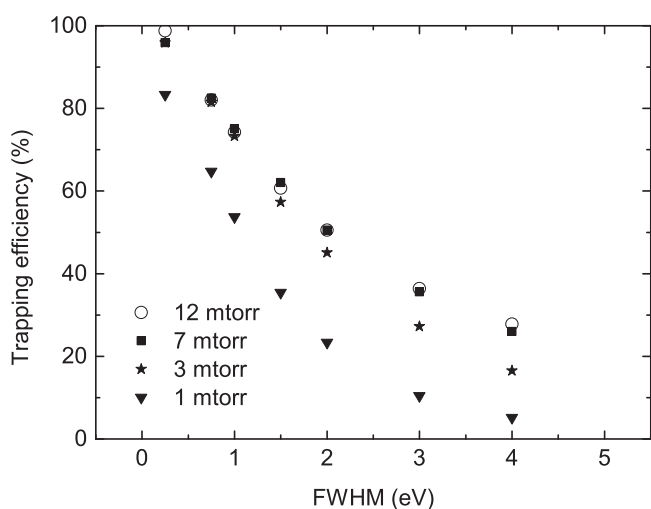
Figure 10. Simulated number efficiency of the trap as a function of the initial energy distributions at different pressures of CF_4 in the first stage.

captured or backscattered. This leads to saturation at pressures over 5 mTorr where 40% of particles are backscattered.

Different positron trap systems in use around the world [11–13, 37, 48] have different properties, including the incident beam parameters. In general the width of beam energy distribution is determined by the moderator properties and is not easily changed. In N_2 traps the positron energy spread is not a critical parameter because the trapping window is so large (see figure 2). However, in a CF_4 trap it is more important because it determines the acceptance of the inlet potential relative to the beam transport energy. In figure 10 we show the simulated CF_4 trap efficiency for different initial beam energy distributions and gas pressures in stage I. As expected, a large beam energy width greatly diminishes the performance of the trap.
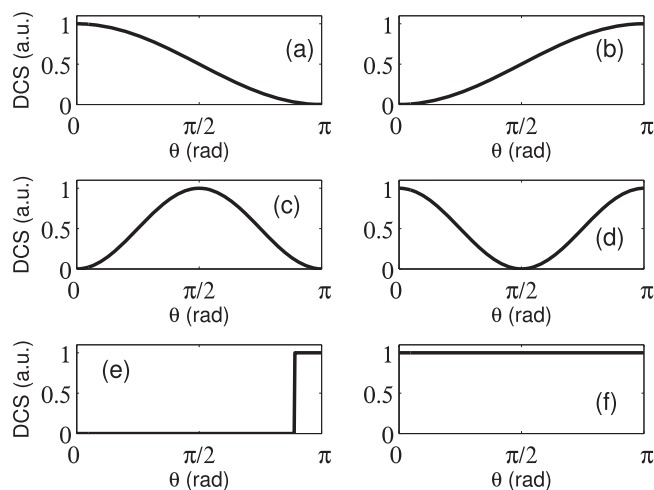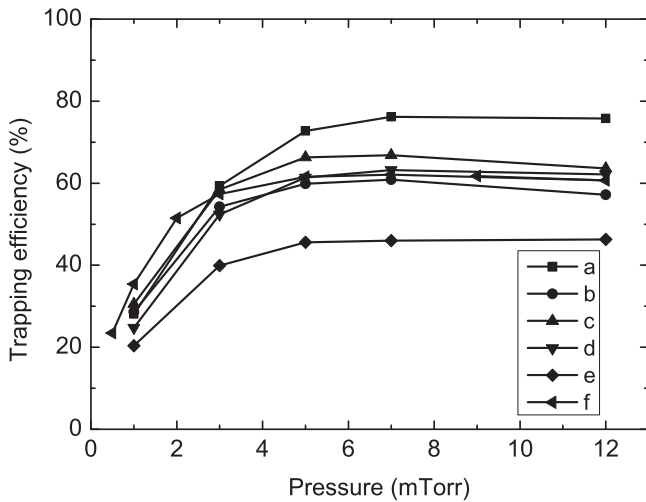

Figure 11. Different model differential scattering cross-sections for elastic scattering of positrons on CF_4.

4. Differential scattering

As discussed in the previous section, the high pressures required for efficient cooling in a CF_4 based buffer-gas trap will give rise to significant beam scattering. In particular, backscattering events can cause particles to leave the trap, becoming the primary loss mechanism. To properly model the backscattering process requires a complete set of DCS, which unfortunately are not currently available. While the direct measurement of DCS for positron-CF_4 interactions is difficult, it can be observed in experiments that the vibrational scattering of positrons on CF_4 at these energies is mostly forward directed. There have also been comparisons between electron and positron vibrational scattering, and it was concluded that the Borne approximation for positrons holds rather well at low energies [50]. However, the relationship between electron and positron elastic scattering cross-sections at these low energies is less straightforward. In order to investigate how robust our model is to different types of differential scattering we have used the Borne dipole approximation [51] cross-section as an estimate for all vibrational excitations. For elastic collisions we have constructed several modal cross sections, including (a) 'forward', (b) 'backward', (c) 'forward–backward', (d) '90°', and for the worst-case scenario (e) 'strongly backward'. Isotropic scattering (f) is included for easier comparison with previous data. These derived cross-sections are shown in figure 11. While there is ample empirical evidence to suggest that the real DCS will be closer to case (a) than anything else, in the absence of measured cross-sections we have investigated the other cases for completeness.

We have performed simulations utilising all of the DCS models shown in figure 11. We find that, for all models, the efficiency saturates at a maximum gas pressure of ∼7 mTorr in stage I. Even in the (highly improbable) worst case scenario (e), an efficiency of ∼40% is obtained for pressures over ∼7 mTorr. As shown in figure 12, the trap efficiency will depend on the shape of the elastic DCS. For the forward

Figure 12. Efficiency of the proposed trap design versus pressure of CF_4 in the first stage for different models of differential scattering cross-sections for elastic scattering of positrons on CF_4. The labels in the legend correspond to different DCS, as shown in figure 11.

scattering case, which is likely to be the most realistic, the trap efficiency could be as high as 75%.

5. CF_4 trapping in an existing N_2 device

Simulations of CF_4 traps indicate that they may offer some significant advantages over the N_2 systems presently used. In particular, increasing trap efficiencies is very desirable considering the cost of producing positron beams. Increasing the number of positrons available is also very important for many experiments, but sources with activities above 50 mCi (1.85 GBq) are not currently available. Therefore, to increase the number of positrons available in trap-based experiments, the only options are (1) to conduct measurements at a high-flux positron facility, such as the reactor-based beam in Munich [52], (2) to construct multiple source-based beams and merge them in one trap, (3) to increase the primary moderator efficiency, or (4) to increase the trap efficiency. Options 1–3 are generally unsatisfactory: beam time is always limited at user-facilities, making long-term research programs difficult; constructing multiple source-based positron beams would be prohibitively expensive; despite many attempts over several decades (e.g., [53]), the efficiency of the solid-neon moderator has not yet been surpassed. Thus, improved trap efficiencies would clearly be highly beneficial. However, there are some experimental challenges that must first be met before the potential of such devices can be realised.

One of the main difficulties in implementing the CF_4 trap is that the energy loss per collision via vibrational excitations (~160 meV) is much smaller than the energy spread of the beam (1.5 eV). Therefore, in order to ensure complete beam capture in the trap multiple collisions are required in the first pass. Conversely, in the N_2 case the energy loss is so large (8.5 eV) that only one excitation event is required, allowing for subsequent cooling to occur on a much longer time scale.

Moreover, by removing such a large amount of energy in a single event, N_2 based traps are less sensitive to the energy spread of the incident positron beam, and can tolerate a significant difference in the magnetic field strength in the trap compared to the source region. The latter point is important because a stronger magnetic field at the trap inlet leads to the transfer of parallel to perpendicular energy (and hence a larger parallel energy spread) owing to conservation of E_{perp}/B, where E_{perp} is the perpendicular positron energy and B is the magnetic field strength (e.g., [54]). Since it is the parallel energy that determines if positrons can traverse the inlet potential step or not, increasing the parallel energy spread in this way necessitates lowering the inlet potential barrier, and hence even more collisions are required to achieve beam capture in one pass.

Since N_2 traps are relatively insensitive to the effects of increasing the perpendicular energy, they tend to be designed with a significant difference in the magnetic field strength between the source and trap (typically a factor of five or more) [8]. This reduces the cost and facilitates beam deflection through an offset aperture to provide more compact radiation shielding. However, this is not the correct way to operate a CF_4 based device, since in this case the beam energy must be kept below the Ps formation threshold (see figure 3), and increasing the parallel energy spread requires more collisions for complete trapping. Nevertheless, we have attempted to test the CF_4 trapping scheme in the UCL two-stage Surko trap [37], shown schematically in figure 13. This was done simply by switching the gas feeds, so that CF_4 was injected directly into stage I, and the electrode potentials were tuned to a configuration similar to that shown in figure 4.

Simulations of this specific trap arrangement (including the different source and trap magnetic fields and the annular beam profile) predicted around $1/3$ of the trapping efficiency usually obtained with N_2 operation (see figure 15). However, no trapping was observed with the system configured for CF_4 operation. This may indicate an increased sensitivity to misalignments or other physical imperfections, or that some additional loss mechanism has been overlooked. In order to investigate this we have performed a series of measurements designed to verify particular aspects of the simulation. Including the real trap geometry and the measured beam energy spread we obtain a simulated efficiency of 6% for N_2 operation.

To determine the parallel energy distribution of the incident positron beam two sets of retarding field measurements were performed. The first used the stage I electrode, which is in the ~565 Gauss magnetic field region, as an analyser. The second used a grid electrode, placed after the trap gate, in a magnetic field of ~110 Gauss. For both measurements the beam energy was 32 eV, and the magnetic field at the source was ~75 Gauss. All electrodes (apart from the analyser) were grounded and no gas was introduced into the system. The measurements and corresponding simulations are shown in figure 14, and exhibit satisfactory agreement. The observed beam energy spread is much larger than the optimal trapping window for N_2 (see figure 2), which contributes significantly to the low trap efficiency.
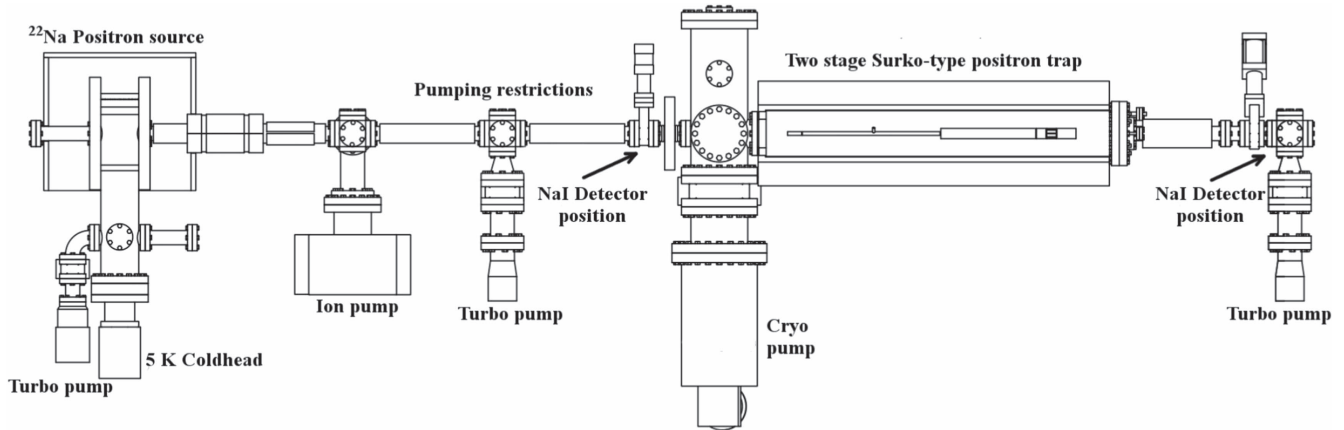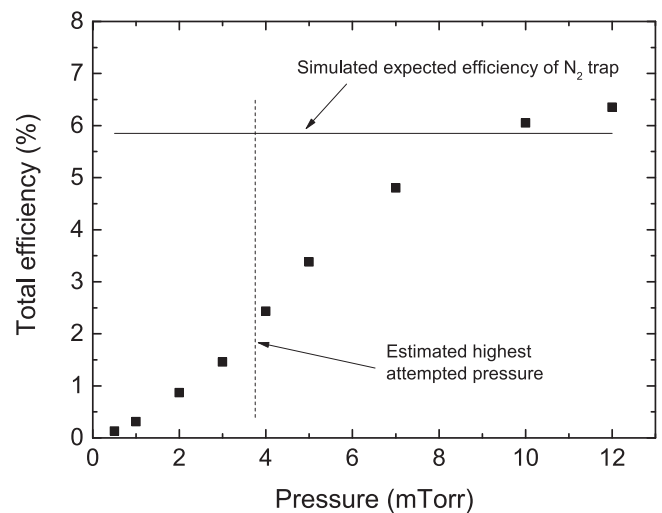
Figure 13. Schematic of the UCL positron beam and trap. Two NaI detector positions are indicated, which are used to monitor the positron beam before (left) and after (right) it passes through the trap electrode structure. The magnetic field in the source region is 75 G and is 565 G in the trap.
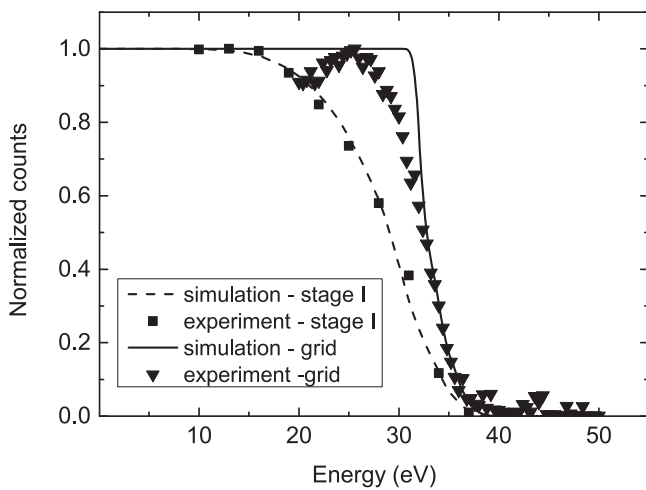
Figure 14. Measured and simulated retarding potential profiles, obtained from the stage I electrode at 565 Gauss and from the grid electrode, placed at the exit of the trap, at 110 Gauss.

Figure 15. Simulated total trapping efficiency versus pressure of CF_4 in the first stage. Simulation included the fitted source energy distributions shown in figure 14 and the effect of E_{perp}/B conservation.

These fitted energy distributions were used in trap simulations which considered the difference in magnetic fields and transport of positrons into the trap, as well as the trapping process, with parameters specific to the experimental arrangement. Therefore, whereas the simulations described in sections 3 and 4 considered only positrons that entered the trap, the simulations presented in figure 15 normalise total efficiency to the number of positrons emitted from the source. Figure 15 presents simulated expected total trapping efficiency using the CF_4 scheme for different pressures of CF_4 in the trapping stage. The horizontal line represents the simulated efficiency of the standard N_2 trap representing the number of particles that is regularly measured. The vertical dashed line represents the maximum pressure for which the trapping was attempted (operating the trap at higher pressures affects the moderator). The reduction in efficiency is a result of the extremely broad axial energy distribution (figure 14): ~70% of positrons backscatter from the inlet electrode, and most of the rest have too much energy to be trapped. Simulations indicate that by increasing the pressure efficiencies

similar to that achieved with N_2 are possible, even for very broad energy distributions. However, even for the highest attempted CF_4 pressure, for which simulations predict 1/3 of regularly achieved positron number, no measurable trapping was observed.

To investigate the attenuation of the beam due to interactions with CF_4 gas, the transmitted fraction was recorded with an NaI detector placed at the trap exit (see figure 13) with all electrodes at ground potential. These data were taken as a function of the beam energy with different amounts of gas present, as shown in figure 16. The data obtained with no added gas demonstrate that there is a minimum energy (~20 eV) required to efficiently transport the beam from the source. When gas is introduced we observe a strong attenuation of the positron beam. However, as is evident from the data, the decreased transmission coincides with the expected Ps formation threshold (~9.45 eV). Thus, the observed beam attenuation is in general not indicative of
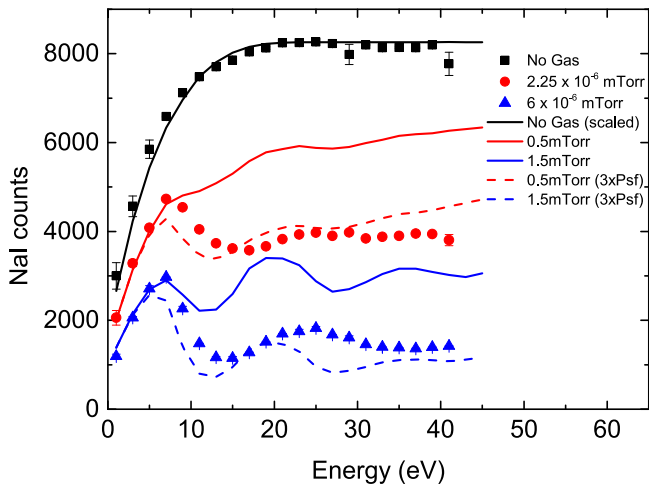
Figure 16. Measured beam transport through grounded trap electrodes with and without CF_4 present at measured pressures indicated in the legend (symbol data). Solid lines represent simulations of transport with stage I pressure indicated in the legend, using CF_4 cross-section set described in [42]. Dashed lines represent simulations of transport with Ps formation scaled up by a factor of 3.
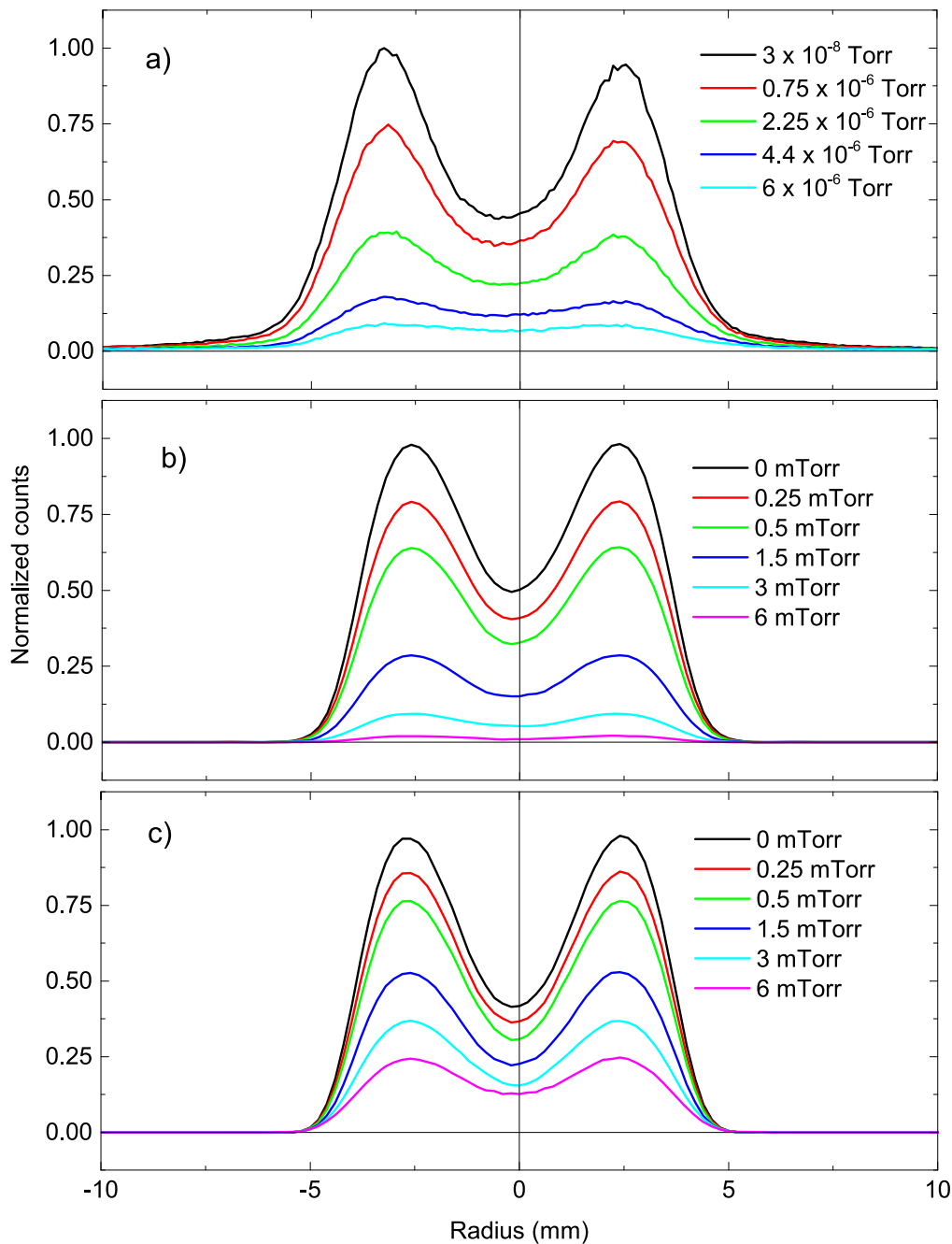

Figure 17. 2D profile of the measured (a) and simulated (b) DC beam. Distortions in the measured beam profile are primarily due to the steering fields between the trap and the imaging detector.

efficient energy loss due to vibrational excitation. The stated pressures are measured in the main trap chamber above the cryo pump, and the actual pressure in the stage I electrode has to be inferred from the expected differential pumping between the two locations. We estimate that the measured pressure is on the order of 500 times lower than that inside stage I.

Simulations of positron beam attenuation when gas is introduced to the trap at two different pressures are presented in figure 16. The losses in the simulation come from either backscattering, transport to the walls, or Ps formation. A simulation with no gas was normalised to the measurements. Assuming uniform differential scattering we have obtained the pressure values that provide a good fit (solid lines) for the data at lower values of the source bias voltage where losses to backscattering and transport to the walls are dominant. The pressures obtained (0.5 and 1.5 mTorr) are somewhat lower than we expect (1.1 mTorr and 3 mTorr respectively) from the ~500 scaling factor estimated from the differential pumping, possibly indicating that the scattering is more forward directed than assumed.

Only total and ionisation cross-section measurements have been performed at the higher energies (i.e., above 10 eV or so), and so the Ps formation cross sections have been estimated from the argon cross-section set, with the threshold shifted to the appropriate value (as explained in [42]). The poor agreement between the simulations and measurements above ~10 eV suggests that the simulated losses to Ps formation may not be strong enough. Figure 16, shows simulations (dashed lines) in which the Ps formation cross-section is increased by a factor of 3, exhibiting improved agreement with the data. It is evident from both experiments and simulations that beam transport into the trap at low source bias voltages is far worse at the energies required for CF_4 trapping scheme (~2 eV) than at the standard operating voltages, due to the difference in magnetic field strength. The addition of
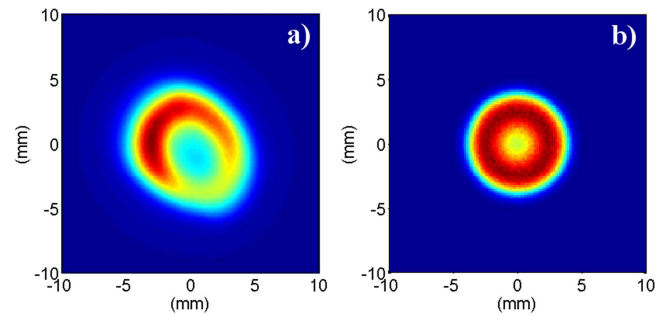
gas further deteriorates the loading efficiency by attenuating the beam through backscattering processes.

The spatial profile of the transmitted DC beam was directly imaged with a microchannel plate detector and CCD camera. The beam profile is significantly different from the flat-top distribution used in the simulations, as shown in figure 17(a). This is due to the conical geometry of the moderator substrate, which results in a toroidal beam profile with an outer diameter of ~8 mm [37]. The measured beam profile is distorted due to slight misalignments between the transport and trapping magnetic fields. It is possible to tune the latter so as to obtain an undistorted image, but with a slightly reduced trapping efficiency. Thus, the observed distortion in the image is not thought to be representative of the actual beam profile inside the trap, and was not included in the simulations (see figure 17(b)).

Owing to the large parallel beam energy spread (see figure 14) it was not possible to perform these measurements with the electrode potential structure properly configured for CF_4 trapping, as this would have rejected most of the incident beam. Instead the source bias and inlet electrodes were operated at 50 V and 39 V respectively, therefore Ps formation was not excluded. 2D beam profiles were obtained (using the $x = y$ diagonal) for different CF_4 pressures, as shown in figure 18(a); the corresponding simulations (utilising the same electrode potentials) are shown in figure 18(b). The simulation shown in figure 18(c) corresponds to source bias and inlet voltages of 41 and 39 V respectively, which should be suitable for CF_4 trapping. Both measurements and simulations were normalised to the corresponding 'no gas' conditions.

In both the measurements and the simulations we observe a significant loss in the beam intensity, and the initial profile is converted to a more uniform distribution. The central region is observed to fill in as the gas pressure is increased, but the overall radial width does not appear to increase. Simulations at the highest pressure (in figure 18(b)), where almost the entire beam is lost (over 97%), reveal that 73% of the those losses are due to Ps formation, 20% being positrons backscattered over the inlet electrode, with less than 7% scattered into the electrode wall. Simulations for 11 eV incident beam energy fit the measured data quite well, using the 500 scaling factor for the pressure. We note that using an incident positron beam with a more Gaussian-like spatial

Figure 18. Measured (a) and simulated (b), (c) line profiles of the DC positron beam for different pressures of CF_4 in the first stage. In (a) and (b) the source/inlet voltages are 50/39 V with the rest of the electrodes set up for CF_4 trapping (similar to figure 4). In (c) source/inlet voltage is 41/39 V which is suitable for CF_4 trap operation.

profile would reduce some of the scattering losses. The annular profile is a result of the particular design of the moderator, which is used because a conical substrate offers improved efficiency [55]. However, it is possible to freeze the Neon gas directly on the ^{22}Na source capsule (e.g., Vasumathi *et al* [56]), with some reduction in the beam intensity.

Simulations were also performed using the correct CF_4 electrode configuration, as shown in figure 18(c). These simulations correspond to the first few points of measurements in figure 14. In this case we find a loss in intensity (compared to the simulation without gas) with increasing gas

pressure that is due almost entirely to scattering in the first stage. At the 6 mTorr pressure required for trapping the total losses amount to 70% of the original beam, where 85% of those losses are backscattered positrons with the remaining 15% of the lost positrons scattered to walls. The 8 mm beam size is close to the 10 mm first stage electrode inner diameter, which increases the likelihood that scattering in the first stage will result in losses on the electrode walls. This simulation, which excludes Ps formation, indicates that the high CF_4 pressures required for efficient energy loss will result in some

Table 2. Estimated total positron trapping efficiency for different moderators and simulated trapping efficiencies.

Moderator and trap	ϵ_{mod} (%)	ΔE (eV)	ϵ_{trap} (%)	ϵ_{total} (%)	e^+/s [4]
Ne [4] and CF$_4$ trap	0.7	1.5	~60	0.42	7.0×10^6
Ne [4] and N$_2$ trap	0.7	1.5	~20	0.14	2.3×10^6
W cone [57] and CF$_4$ trap	0.15	75×10^{-3}	>90	0.135	2.2×10^6
W vanes [58] and CF$_4$ trap	0.07	75×10^{-3}	>90	0.063	1.0×10^6
W(100) foil [59] and CF$_4$ trap	0.06	75×10^{-3}	>90	0.054	0.9×10^6
W cone [57] and N$_2$ trap [9]	0.15	75×10^{-3}	~30	0.045	7.5×10^5
W foil [60] and CF$_4$ trap	0.026	75×10^{-3}	>90	0.0234	3.9×10^5

[4] Estimated number of trapped positrons per second based on a 50 mCi Na^{22} source.

additional beam loss in an electrode geometry suitable for N$_2$ trapping.

6. Discussion and conclusions

We have formulated a model of a positron trap that uses CF$_4$ as the primary buffer gas, and have carried out Monte Carlo simulations to investigate the efficacy of such an arrangement. The idea behind the design is conceptually straightforward, namely to trap using vibrational excitations of CF$_4$ instead of electronic excitations of N$_2$, and thereby avoid losses due to Ps formation. In reality this straightforward scheme is difficult to implement because of the low energy loss per vibrational excitation (~160 meV), which means that many collisions are required to ensure positron capture. Furthermore, the trapping efficiency is very sensitive to the energy spread of the incident positron beam, a problem that is seriously exacerbated by typical magnetic field configurations. Nevertheless, the simulations predict that trapping efficiencies of the order of 60% may be obtainable using this approach. Since the proximity of the excitation and Ps formation cross-sections in N$_2$ results in a fundamental limitation in the efficiency on the order of 25%, this would be beneficial.

A CF$_4$ based trap would be limited by losses due to backscattering, owing to the high gas pressures required. The extent of this effect is evident in figure 12, and limits efficiencies to approximately 45%–75%. Other complications can in principle be overcome by appropriate engineering of the device, optimising gas pressures, electrode radii and applied voltages. The operation of a real trap will depend upon the incident positron beam properties to a much greater extent than is the case for an N$_2$ based system, and so trap design should take this into account.

The measurements suggest that the main obstacle preventing the direct re-purposing of N$_2$ traps to CF$_4$ use is the difference in the magnetic field strength in the source and trap regions. The broad kinetic energy distributions caused by this result in either reflecting a large portion of the incident positrons (by setting the inlet voltage too high), or reduced trapping efficiency (by setting it too low). Thus, for a CF$_4$ device to work efficiently, the trap and source magnetic fields need to be appropriately matched. This is generally not done in N$_2$ systems, simply because it is not necessary. Solving this problem is straightforward, but does require some redesigning

of the system, as opposed to re-purposing existing N$_2$ traps. However, it is, in essence, an engineering problem, whereas the Ps losses inherent in N$_2$ traps is physical in nature.

Even in a device perfectly engineered for CF$_4$ trapping, some advantage might be gained by using a tungsten moderator, which provides much narrower positron energy distributions than solid neon [2, 38, 57]. Increasing the trapping efficiency in this way comes at the cost of the primary beam intensity, so one must consider several parameters simultaneously when evaluating such options. The simulations indicate that with the narrow energy distributions typical of tungsten moderators, higher trap efficiencies might be obtained (see figure 10). Furthermore, tungsten moderators do not require cryogenic temperatures, and are thus significantly cheaper and easier to implement than solid neon. In some cases reducing the cost and complexity of a beam and trap system, while maintaining the total throughput of accumulated positrons, would be an appropriate strategy. However, in terms of maximising the overall number of positrons available, it would remain beneficial to use a Neon moderator, even with a fully optimised CF$_4$ based trap (see table 2). It may also be possible to use a Neon moderator and a tungsten remoderator together; reflection-mode remoderation efficiencies of the order of 25% have been reported [2], although in principle 50% is possible. If real operating conditions, more complex geometries and other factors led to only a 25% efficiency then the Ne + W arrangement would give 0.18%, which would be comparable to a W cone (0.15%) and probably not worth the effort. On the other hand, these efficiency numbers are all idealised, and making distinctions based on factors of two can hardly be justified. It is likely that remoderating Neon-based beams would be advantageous, even when using a standard N$_2$ trap (especially if the magnetic field discrepancy between source and trap is large).

The primary goal of this work was to evaluate the efficacy of a CF$_4$ based trap using a numerical Monte Carlo code to simulate the operation of such a device, incorporating measured cross-sections (where possible) and realistic device parameters. We conclude that an appropriately designed CF$_4$ trap could operate with efficiencies ranging from 60% to 90%, depending on the type of moderator used. We also demonstrated that designs suitable for N$_2$ traps are generally not capable of operating as CF$_4$ devices, mostly because of the mismatch between the source and trap magnetic fields.

Acknowledgments

References

[1] Canter K F, Coleman P G, Griffith T C and Heyland G R 1972 *J. Phys. B: At. Mol. Phys.* **5** L167
[2] Shultz P J and Lynn K G 1988 *Rev. Mod. Phys.* **60** 701
[3] Coleman P G 2000 *Positron Beams and Their Applications* ed P G Coleman (Singapore: World Scientific)
[4] Mills A P Jr and Gullikson E M 1986 *Appl. Phys. Lett.* **49** 1121
[5] Charlton M and Humberston J 2000 *Positron Physics* (New York: Cambridge University Press)
[6] Crompton R W 1994 *Adv. At. Mol. Opt. Phys* **33** 97
[7] Surko C M, Leventhal M and Passner A 1989 *Phys. Rev. Lett.* **62** 901
[8] Danielson J R, Dubin D H E, Greaves R G and Surko C M 2015 *Rev. Mod. Phys.* **87** 247
[9] Murphy T J and Surko C M 1992 *Phys. Rev. A* **46** 5696
[10] Surko C M and Greaves R G 2004 *Phys. Plasmas* **11** 2333
[11] Clarke J, van der Werf D P, Griffiths B, Beddows D C S, Charlton M, Telle H H and Watkeys P R 2006 *Rev. Sci. Instrum.* **77** 063302
[12] Sullivan J P, Jones A, Caradonna P, Makochekanwa C and Buckman S J 2008 *Rev. Sci. Instrum.* **79** 113105
[13] Cassidy D B, Deng S H M, Greaves R G and Mills A P 2006 *Rev. Sci. Instrum.* **77** 073106
[14] Marler J P and Surko C M 2005 *Phys. Rev. A* **72** 062713
[15] Marler J P and Surko C M 2005 *Phys. Rev. A* **72** 062702
[16] Marler J P, Sullivan J P and Surko C M 2005 *Phys. Rev. A* **71** 022701
[17] Makochekanwa C *et al* 2009 *New J. Phys.* **11** 103036
[18] Cassidy D B, Hisakado T H, Tom H W K and Mills A P Jr 2012 *Phys. Rev. Lett.* **108** 133402
[19] Andresen G B *et al* 2010 *Nature* **468** 673
[20] Amoretti M *et al* 2002 *Nature* **419** 456
[21] Gabrielse G *et al* 2002 *Phys. Rev. Lett.* **89** 213401
[22] Cassidy D B, Crivelli P, Hisakado T H, Liszkay L, Meligne V E, Perez P, Tom H W K and Mills A P Jr 2010 *Phys. Rev. A* **81** 012715
[23] Platzman P M and Mills A P Jr 1994 *Phys. Rev. B* **49** 454
[24] Banković A, Dujko S, White R D, Marler J P, Buckman S J, Marjanović S, Malović G, Garcia G and Petrović Z L 2012 *New J. Phys.* **14** 035003
[25] Banković A, Petrović Z L, Robson R E, Marler J P, Dujko S and Malović G 2009 *Nucl. Instrum. Meth. B* **267** 350
[26] Šuvakov M, Petrović Z L, Marler J P, Buckman S J, Robson R E and Malović G 2008 *New J. Phys.* **10** 053034
[27] Banković A, Marler J P, Šuvakov M, Malović G and Petrović Z L 2008 *Nucl. Instrum. Meth. B* **266** 462
[28] Banković A, Dujko S, White R D, Buckman S J and Petrović Z L 2012 *Nucl. Instrum. Meth. B* **279** 92

[29] Petrović Z Lj, Marjanović S, Dujko S, Banković A, Malović G, Buckman S, Garcia G, White R and Brunger M 2014 *Appl. Rad. Isotop.* **83** 148
[30] Marjanović S, Šuvakov M, Banković A, Savić M, Malović G, Buckman S J and Petrović Z L 2011 *IEEE Trans. Plasma Sci.* **39** 2614
[31] Greaves R G and Moxom J 2003 *AIP Conf. Proc.* **692** 140
[32] Oshima N, Kojima T M, Niigaki M, Mohri A, Komaki K and Yamazaki Y 2004 *Phys. Rev. Lett.* **93** 195001
[33] Estrada J, Roach T, Tan J N, Yesley P and Gabrielse G 2000 *Phys. Rev. Lett.* **84** 859
[34] Natisin M R, Danielson J R and Surko C M 2014 *J. Phys. B: At. Mol. Phys.* **47** 225209
[35] Banković A, Dujko S, Marjanović S, White R D and Petrović Z L 2014 *Eur. Phys. J. D* **68** 127
[36] Natisin M R, Danielson J R and Surko C M 2016 *Appl. Phys. Lett.* **108** 024102
[37] Cooper B S, Alonso A M, Deller A, Wall T E and Cassidy D B 2015 *Rev. Sci. Instrum.* **86** 103101
[38] Fischer D A, Lynn K G and Gidley D W 1986 *Phys. Rev. B* **33** 4479
[39] Kurihara M, Petrović Z L and Makabe T 2000 *J. Phys. D: Appl. Phys.* **33** 2146
[40] Murtagh D J 2014 *Eur. Phys. J. D* **68** 213
[41] Petrović Z L *et al* 2014 *J. Phys. Conf. Ser* **488** 012047
[42] Petrović Z L, Banković A, Dujko S, Marjanović S, Malović G, Sullivan J P and Buckman S J 2013 *AIP Conf. Proc.* **1545** 115
[43] Raspopović Z M, Sakadžić S, Bzenić S and Petrović Z L 1999 *IEEE Trans. Plasma Sci.* **27** 1241
[44] Petrović Z L, Raspopović Z M, Dujko S and Makabe T 2002 *Appl. Surf. Sci.* **192** 1
[45] Dujko S, Raspopović Z M and Petrović Z L 2005 *J. Phys. D: Appl. Phys.* **38** 2952
[46] Ristivojević Z and Petrović Z L 2012 *Plasma Sour. Sci. Technol.* **21** 035001
[47] Petrović Z L, Dujko S, Marić D, Malović G, Nikitović Ž, Šašić O, Jovanović J, Stojanović V and Radmilović-Radenović M 2009 *J. Phys. D: Appl. Phys.* **42** 194002
[48] Greaves R G and Surko C M 2002 *Nucl. Instrum. Meth. B* **192** 90
[49] Greaves R G and Moxom J M 2008 *Phys. Plasmas* **15** 072304
[50] Marler J P, Gribakin G F and Surko C M 2006 *Nucl. Instrum. Meth. B* **247** 87
[51] Mann A and Linder F 1992 *J. Phys. B: At. Mol. Opt.* **25** 545
[52] Hugenschmidt C, Piochacz C, Reiner M and Schreckenbach K 2012 *New J. Phys.* **14** 055027
[53] Brandes G R, Canter K, Krupyshev A, Xie R and Mills A P 1997 *Mater. Sci. Forum* **255-257** 653
[54] Davidson R C 2001 *Physics of Non-Neutral Plasmas* (London: Imperial College Press)
[55] Khatri R, Charlton M, Sferlazzo P, Lynn K G, Mills A P Jr and Roellig L O 1990 *Appl. Phys. Lett.* **57** 2374
[56] Vasumathi D, Amarendra G, Canter K F and Mills A P Jr 1995 *Appl. Surf. Sci.* **85** 154
[57] Lynn K G, Gramsch E, Usmar S G and Sferlazzo P 1989 *Appl. Phys. Lett.* **55** 87
[58] Dale J M, Hulett L D and Pendyala S 1980 *Surf. Interface Anal.* **2** 199
[59] Lynn K G, Nielsen B and Quateman J H 1985 *Appl. Phys. Lett.* **47** 239
[60] Gramsch E, Throwe J and Lynn K G 1987 *Appl. Phys. Lett.* **51** 1862